

**WATER ICE CLOUDS IN THE MARTIAN ATMOSPHERE: A COMPARISON OF TWO METHODS**

**AND ERAS** A.S. Hale<sup>1</sup>, L.K. Tamppari<sup>1</sup>, P. R. Christensen<sup>2</sup>, M. D. Smith<sup>3</sup>, Deborah Bass<sup>1</sup> and J. C. Pearl<sup>3</sup>, <sup>1</sup>Jet Propulsion Laboratory/California Institute of Technology, M/S 264-235, 4800 Oak Grove Dr., Pasadena, CA 91109, amy.s.hale@jpl.nasa.gov, <sup>2</sup>Arizona State University, Dept. of Geology, Box 871404, Tempe, AZ 85287-1404, <sup>3</sup>NASA Goddard Space Flight Center, Mail Code 693, Greenbelt, MD 20771.

**Introduction:** Over the past decade there has been an increased interest in water-ice clouds in the Martian atmosphere and the role they may play in the water cycle. Water-ice clouds in the Martian atmosphere have been inferred, historically, through observations of “blue” and “white” clouds [1], but the first positive confirmation of water-ice in the atmosphere came during the Mariner 9 mission, through the Infrared Interferometer Spectrometer experiment [2]. Subsequent data sets have continued to show evidence for water ice clouds.

More recently, work has suggested that clouds forming in a low-latitude belt during the northern spring/summer time frame (the aphelion cloud belt) may be retaining water in and scavenging water to the northern hemisphere [3,4]. This cloud belt forms during northern spring/summer. At the current epoch, Mars’ northern spring/summer timeframe coincides with aphelion ( $L_s=71^\circ$ ), causing the atmospheric temperatures to be lower in this season, allowing water-ice clouds to form more readily than during the perihelion season. Ice particles in the clouds may gravitationally settle, confining water to the northern hemisphere. This settling may also remove dust acting as cloud condensation nuclei, decreasing the radiative heating potential of the atmosphere further. This is a powerful mechanism to explain why Mars’ northern hemisphere contains substantially more water than the southern hemisphere.

Furthermore, the aphelion cloud belt was not originally recognized as an annual feature in the Martian climate and was originally proposed to be due to a climate change since Viking [3]. However, Viking data did show the aphelion cloud belt over two Martian years [5], as well as widespread and frequent water ice clouds throughout the Martian year. Water ice clouds, and specifically the aphelion cloud belt, have also been seen through the MGS TES data set [6-10]. Since this belt is now seen as most likely an annual feature of the Martian climate, it is desirable to understand its characteristics, such as its spatial and temporal extent, and variations in opacity, temperature, and altitude. To date, the only two data sets offer the potential to examine year-to-year changes in cloud features over an entire Martian year: the Viking Infrared Thermal Mapper (IRTM) data set [5] and the Mars Global Sur-

veyor (MGS) Thermal Emission Spectrometer (TES) data set [6-10]. We have examined the TES data in the same way in which we examined the Viking IRTM data [5; 9-10] This provides water-ice cloud information separated in time by 12 Martian years. Since the data are analyzed with the same method, we obtain a very accurate “apples to apples” comparison, and can generate a historical record of the subtleties of this annual event. However, the methodology used in our retrievals of water-ice clouds from TES data differs from the methodology used by [6-8]. Consequently, it is desirable to compare their results to ours to see what differences exist, and better assess the strengths of both methods.

**Method:** To assess the true extent of the interannual variability in water-ice cloud formation, a direct and robust method for comparing these different data sets and time periods has been used [5]. The water-ice cloud retrieval technique developed to analyze the broadband Viking IRTM channels [5] has been applied to the TES data. To do this, the TES spectra are convolved to the IRTM bandshapes and spatial resolutions, enabling the same processing techniques as were used in Tamppari *et al.* [5]. The resulting cloud maps are therefore directly comparable to those created for the Viking time period. This method is powerful, but it cannot be applied over cold surfaces, as it relies on sensing a cold cloud over a warmer surface. Therefore, areas of the surface which the surface model expects to be cold are explicitly ignored. Figure 1 a and b show a typical result for MGS TES and Viking IRTM. Others [6-8] have determined water-ice opacities from the TES spectra by first computing a column integrated opacity for pure atmospheric absorbers as a function of wavenumber, and then estimating the water ice contribution by simultaneously fitting predetermined spectral shapes for atmospheric dust, water ice, as well as non-unit surface emissivity. The method also assumes that the absorber, in this case water ice, is well mixed in the atmospheric column, an assumption that may not be correct. This method also becomes noisy over cold surfaces, but can still be applied. Figure 2 shows a map for the same  $L_s$  range and Martian year as figure 1a in opacity data, though it includes a larger latitude range. The large opacity signature at high southern latitude is real; analysis of MOC images in this time frame [11]

show cloud cover in the areas of high opacity, but these images cannot tell us the composition of the clouds beyond the fact that they are condensate and not dust. Since this clouded area is part of the southern polar hood, it may also contain  $\text{CO}_2$  as well as water ice clouds. It should be noted that the color scale on figures 1 and 2 are not the same. In figure 1, blue indicates water ice clouds, whereas in figure 2 redder areas indicate areas of high water ice opacity.

**Conclusions: Method Comparison:** Similar cloud features are seen in maps generated with each method with no obvious outliers. The temperature differencing method appears to possibly be somewhat more sensitive to weaker water ice signatures. We have also generated correlation plots comparing the two methods (figure 3). At strong delta-T signals, the correlation between the two methods is quite good, and therefore extraction of opacities from earlier Viking data may be possible for these stronger detection levels. Weaker detections do not, however, show such a good correlation. We are currently analyzing why the correlation becomes poor at weak signal levels, though it may be due to the fact that the differencing method may be more sensitive to thin cloud hazes. Results of this ongoing analysis will be presented.

**Conclusions: Viking and MGS eras:** While the data coverage is much greater in the TES data set, water-ice cloud maps from the same seasons have similar characteristics to those seen in the Viking dataset. In particular, the aphelion low-latitude cloud belt is prominent, as is the cloud cover over Hellas and the topographic highs. Analysis of the differences and similarities between the results generated by each technique is ongoing. Due to gaps in data coverage, this aphelion cloud belt is not as well seen in this particular Viking map (figure 1b), but it is clearly present. In addition, a strong cloud signature in Figure 1a, indicating either a colder or thicker water-ice cloud, is present over Elysium Mons, over the Tharsis volcano region, and over the northern part of Hellas basin. Results in other  $L_s$  ranges are similar; that is, prominent features seen by Viking are also observed by MGS, though of course coverage in the Viking data is less extensive.

**References:** [1] Slipher, E. C. (1962) *Mars*, Northland Press. [2] Curran, R. J. et al. (1973) *Science*, 183, 381-383. [3] Clancy, R. J. et al. (1996) *Icarus*, 122, 36-62. [4] Richardson, M. I., et al. (2003) *JGR*, 107, 5064- 5093. [5] Tamppari, L. K. et al. (2000) *JGR*, 105 4087 - 4107. [6] Smith, M. D et al. (2001) *GRL*, 28, 4263-4266. [7] Smith, M. D. (2001b) et al., *JGR*, 105 9539-9552. [8] Pearl, J. D. et al. (2001) *JGR*, 106, 12325-12338. [9] Hale, A.S. et al. (2002) 34<sup>th</sup> DPS, 15.11. [10] Tamppari, L.K., et al. (2002) 34<sup>th</sup> DPS 06.06. [11] Wang and Ingersoll (2002) *JGR*, 107 E10 1-8.

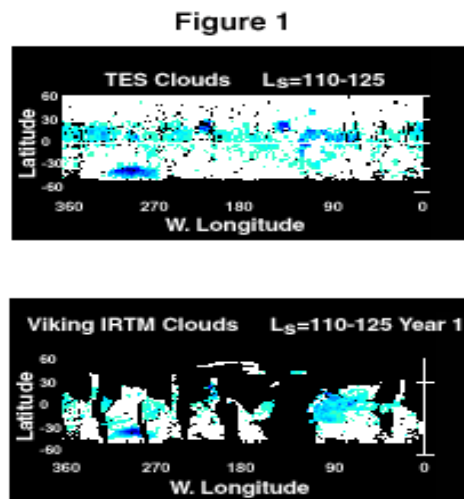


Figure 1: (a) Water ice clouds for  $L_s$  110 – 125 as seen by TES in MGS extended mission. (b) Water ice clouds as seen by Viking IRTM for the same  $L_s$  range. Though coverage in the Viking data is not as complete, similar features are seen.

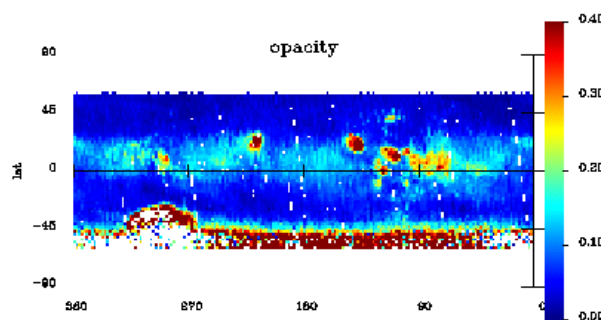


Figure 2: The same  $L_s$  range and era (MGS extended mission) mapped in water ice opacity. Note that the color scale is reversed, with red indicating high water ice opacity, and that a greater latitude range is shown.

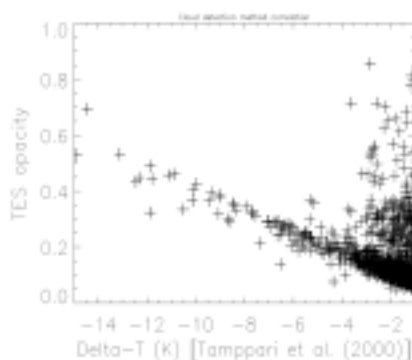


Figure 3: Correlation plot of data from Figure 1a and figure 2. Note the strong correlation at high opacities and delta T values.